THE JOURNAL OF BIOLOGICAL CHEMISTRY VOL. 288, NO. 24, pp. 17932–17940, June 14, 2013

Ferroportin and Exocytoplasmic Ferroxidase Activity Are Required for Brain Microvascular Endothelial Cell Iron Efflux*

Received for publication, January 23, 2013, and in revised form, April 30, 2013 Published, JBC Papers in Press, May 2, 2013, DOI 10.1074/jbc.M113.455428

Ryan C. McCarthy and Daniel J. Kosman[1]

From the Department of Biochemistry, University at Buffalo, School of Medicine and Biomedical Sciences, Buffalo, New York 14214

Background: Cellular iron efflux occurs via cooperation of ferroportin and a ferroxidase.
Results: Depletion of ferroxidase and ferroportin from human brain microvascular endothelial cells decreases their ability to efflux iron.
Conclusion: Iron efflux from brain microvascular endothelial cell ferroportin requires exocytoplasmic ferroxidase activity.
Significance: The mechanism of iron efflux from endothelial cells of the blood-brain barrier is fundamental to how iron enters the brain.

The mechanism(s) of iron flux across the brain microvasculature endothelial cells (BMVEC) of the blood-brain barrier remains unknown. Although both hephaestin (Hp) and the ferrous iron permease ferroportin (Fpn) have been identified in BMVEC, their roles in iron efflux have not been examined. Using a human BMVEC line (hBMVEC), we have demonstrated that these proteins are required for iron efflux from these cells. Expression of both Hp and Fpn protein was confirmed in hBMVEC by immunoblot and indirect immunofluorescence; we show that hBMVEC express soluble ceruloplasmin (Cp) transcript as well. Depletion of endogenous Hp and Cp via copper chelation leads to the reduction of hBMVEC Fpn protein levels as well as a complete inhibition of ^{59}Fe efflux. Both hBMVEC Fpn protein and ^{59}Fe efflux activity are restored upon incubation with 6.6 nM soluble plasma Cp. These results are independent of the source of cell iron, whether delivered as transferrin- or non-transferrin-bound ^{59}Fe. Our results demonstrate that iron efflux from hBMVEC Fpn requires the action of an exocytoplasmic ferroxidase, which can be either endogenous Hp or extracellular Cp.

Several neuronal processes require iron such as myelination, mitochondrial energy generation, cell division, and neurotransmission (1, 2). When not properly regulated, iron can readily form cell-damaging reactive oxygen species via Fenton chemistry (Equation 1) and thus must be tightly regulated by both cellular and extracellular mechanisms.

$$Fe^{II} + H_2O_2 \rightarrow Fe^{III} + OH^{\bullet} + OH^{-} \quad \text{(Eq. 1)}$$

To prevent such free radical formation in blood or the interstitial spaces of the brain, mammals have developed ways to maintain iron in its less reactive Fe^{III} form. To accomplish this, coordination between several iron-related proteins is required to safely export Fe^{III} from cells. Cellular iron efflux occurs through the Fe^{II} transporter ferroportin (Fpn)[2] (3, 4); Fpn has been identified in the brain microvascular endothelial cells (BMVEC) of the blood-brain barrier (BBB) (5, 6). Upon cellular iron efflux through Fpn, Fe^{II} is oxidized by a multicopper oxidase; two such multicopper oxidases exist in mammals, hephaestin (Hp) and ceruloplasmin (Cp) (7–9). Hephaestin is found co-localized and in functional complex with Fpn on the surface of mammalian epithelial cells lining the gut (8, 10, 11). The ferroxidase-generated Fe^{III} becomes bound by a variety of iron-chelators and proteins found in blood, *e.g.* transferrin (Tf), ferritin, and citrate; this same cohort of ferric iron ligands are found in the brain (12). In the brains of sex-linked anemic mice ($sla^{-/-}$), which contain mutations in the Hp gene, iron accumulation has been shown in oligodendrocytes of the gray matter, suggesting a role for Hp in iron efflux from cells of the CNS (9, 13). Although these mice still accumulate brain iron, they likely do so via soluble Cp (sCp) present in the interstitial fluid localized to the abluminal surface of the BMVEC. This sCp can be provided by astrocytes (14) or, as we demonstrate here, by hBMVEC. Hp but not Cp has been reported previously in the BMVEC of the BBB (6, 15, 16).

Brain iron accumulation has been correlated with several neurological diseases, including Alzheimer and Parkinson disease (17, 18). Understanding the mechanism of iron transport across the endothelial cells of the BBB is crucial in developing an understanding of the pathogenesis of these neurological diseases. Currently, the mechanism of iron transport across the endothelial cells of the BBB is poorly understood. In one model, serum Tf-iron is transcytosed across the BMVEC followed by release of Tf-iron or iron alone at the abluminal membrane (18, 19). This model, which has not been experimentally verified, does not account for the uptake by these cells of non-transferrin-bound iron (20). Our goal in this work was to delineate the mechanism of iron efflux from BMVEC; we specifically com-

* This work was supported by Grant DK053820 from the National Institutes of Health (to D. J. K.) and a predoctoral fellowship from the American Heart Association (to R. C. M.).

[1] To whom correspondence should be addressed: Dept. of Biochemistry, University at Buffalo, Farber Hall Rm. 140, 3435 Main St., Bldg. 26, Buffalo, NY 14214-3000. Tel.: 716-829-2842; Fax: 716-829-2661; E-mail: camkos@buffalo.edu.

[2] The abbreviations used are: Fpn, ferroportin; BMVEC, brain microvascular endothelial cell(s); Cp, ceruloplasmin; Hp, hephaestin; GPI-Cp, glycophosphatidylinositol-anchored Cp; hBMVEC, human brain microvascular cell line; BBB, blood-brain barrier; Tf, transferrin; sCp, soluble plasma ceruloplasmin; TBI, transferrin-bound iron; NTBI, non-transferrin-bound iron; BCS, bathrocuproinedisulfonic acid disodium salt.

pared efflux of iron obtained from either Tf-iron (TBI or non-Tf-bound iron (NTBI).

We demonstrate that Fpn and Hp proteins are expressed by human BMVEC (hBMVEC). Furthermore, we report here the presence of the soluble Cp transcript. This is the first example of the existence of the Cp message in the endothelial cells of the BBB. Depletion of endogenous multi-copper oxidase proteins via treatment with the copper chelating agent bathrocuproinedisulfonic acid disodium salt (BCS) demonstrated that hBMVEC iron efflux is dependent upon endogenous Fpn and exocytoplasmic ferroxidase activity. Our results indicate that endogenous Hp and/or sCp can fulfill the role of ferroxidase in this iron efflux pathway. The positive correlation between hBMVEC ferroxidase expression and iron efflux is quantitatively the same irrespective of cell iron loading by TBI or NTBI suggesting that Fpn-dependent efflux predominates in this monolayer system.

EXPERIMENTAL PROCEDURES

Cell Culture and Reagents—hBMVEC were cultured in RPMI 1640 with 10% FBS and 10% NuSerum as described previously (20). Experiments were performed in 33-mm tissue culture dishes or 24-well tissue culture dishes unless otherwise specified. Human soluble plasma ceruloplasmin was purchased from GenWay Biotech, Inc. (San Diego, CA).

Immunoblots—Immunoblots were performed as described previously with minor changes (20). Briefly, hBMVEC were harvested with radioimmune precipitation assay buffer plus protease inhibitors. SDS-PAGE (8%) was used to separate 20 μg of protein per lane. The membrane was blocked 1 h with PBS 3% BSA, incubated with mouse anti-hephaestin (ab56729) or rabbit anti-SLC40A1 (ferroportin) (ab78066) (Abcam, Inc., Cambridge, MA) overnight at 4 °C and then incubated with secondary anti-HRP antibody (Santa Cruz Biotechnology). Blots were adjusted for brightness and contrast using Adobe Photoshop software (version 7.0).

Indirect Immunofluorescence—hBMVEC were fixed for 10 min with 3.7% paraformaldehyde and 4% sucrose in PBS containing 1 mM $CaCl_2$ and 0.5 mM $MgCl_2$. hBMVEC were then blocked and permeabilized for 1 h in PBS 0.1% Tween 20 with 1% BSA and 0.3 M glycine. Cells were then incubated for 30 min with anti-hephaestin (1:100) or anti-SLC40A1 (1:100) in PBS 1% BSA and then incubated for 30 min with Alexa Fluor 488-conjugated donkey anti-mouse or goat anti-rabbit (1:1000, Invitrogen) in PBS 1% BSA. Coverslips were mounted onto glass slides using SlowFade gold antifade reagent with DAPI (Invitrogen). Images from at least five different fields of view were obtained using a Zeiss AxioImager Z1 Axiophot widefield fluorescence microscope and Zeiss AxioVision software (Zeiss, Thornwood, NY). Analyses of relevant fluorescent intensities were performed using Zeiss AxioVision software and Prism (version 4.0, GraphPad Software). All fluorescent intensities were normalized for their respective secondary antibody control fluorescent intensities.

^{59}Fe Accumulation and Efflux Assays—All ^{59}Fe uptake and efflux assays were performed using confluent monolayers of hBMVEC grown in 24-well tissue culture dishes. Assays were performed at 37 °C 5% CO_2 at 75 rpm. The radionuclide $^{59}FeCl_3$ was purchased from Perkin-Elmer Life Sciences. HBMVEC were loaded with $^{59}Fe^{II}$ citrate using a reductase-independent uptake protocol based on the presence of 5 mM dihydroascorbate and 250 μM citrate. Reactions were quenched with ice-cold quench buffer as described previously (20) and lysed with radioimmune precipitation assay buffer. Lysates were assayed for ^{59}Fe and protein concentration. For efflux assays, hBMVEC were loaded for 24 h, washed with RPMI 1640 containing 250 μM citrate, and incubated with reagents as noted in each experiment for 0–24 h. The medium was collected, and the cells were quenched and processed as described above.

RT-PCR—Total RNA was extracted from hBMVEC, C6 glioma cells, or HepG2 cells using the TRIzol reagent (Invitrogen) as per the manufacturer's instructions. After DNase treatment, RNA was reverse-transcribed, and PCR was performed using the Qiagen OneStep RT-PCR kit. Primers used for RT-PCR are listed in Table 1.

Ferroxidase Assays—hBMVEC were lysed with 0.2% Triton X-100 for 1 h at 37 °C 5% CO_2 at 75 rpm. Lysates were concentrated, and 300 μg total protein was used per condition unless indicated otherwise. Assays were performed in 100 mM MES buffer, pH 6, 10 μM freshly prepared ferrous ammonium sulfate for 1 h at room temperature. Ferrozine (100 μM) was used as the colorimetric indicator producing an absorbance at 550 nm when in complex with ferrous iron. All assays were blanked for iron-only controls.

Other Procedures—Apo-Tf (Sigma-Aldrich) was loaded with ^{59}Fe as described previously (20). Efflux of ^{59}Fe resulting from ^{59}Fe-Tf uptake were performed as described for $^{59}Fe^{II}$ citrate. Copper chelation was performed with 500 μM BCS (Sigma-Aldrich) for 24 to 48 h. All statistical analyses were performed by using Prism software (version 4.0). All counts were normalized for protein concentration obtained at time 0 h.

RESULTS

hBMVEC Efflux Iron Accumulated from $^{59}Fe^{II}$ citrate (NTBI) or ^{59}Fe-transferrin (TBI)—We have demonstrated previously that hBMVEC readily import $^{59}Fe^{II}$ citrate (20). Prior to investigating the mechanism of hBMVEC iron efflux, we monitored the accumulation of $^{59}Fe^{II}$ citrate in an effort to establish an end point. The accumulation of $^{59}Fe^{II}$ citrate by hBMVEC appears to plateau after 20 min (Fig. 1*A*, *inset*). However, data collected for up to 24 h indicate that the accumulation of $^{59}Fe^{II}$ citrate by hBMVEC is biphasic in nature (Fig. 1*A*). As the end point for hBMVEC iron accumulation was reached by 24 h, we used this time frame for hBMVEC iron loading in our subsequent experiments.

To establish an end point for iron efflux from hBMVEC, cells were ^{59}Fe-loaded with ^{59}Fe-citrate (NTBI), washed, and incubated with efflux media for 0, 24, or 48 h. hBMVEC exported ^{59}Fe over time, reaching an apparent end point during the first 24 h of the assay (data not shown). hBMVEC lost 35.4 ± 3.2% of their cell-associated ^{59}Fe after 24 h (Fig. 1*B*, *open bar*). Efflux assays were performed also after loading hBMVEC with ^{59}Fe-Tf (TBI). A similar loss of cell-associated ^{59}Fe after 24 h was observed (34.9 ± 0.2%) (Fig. 1*B*, *filled bar*). These data show that hBMVEC accumulate and efflux ^{59}Fe presented in both transferrin-bound and non-transferrin-bound forms.

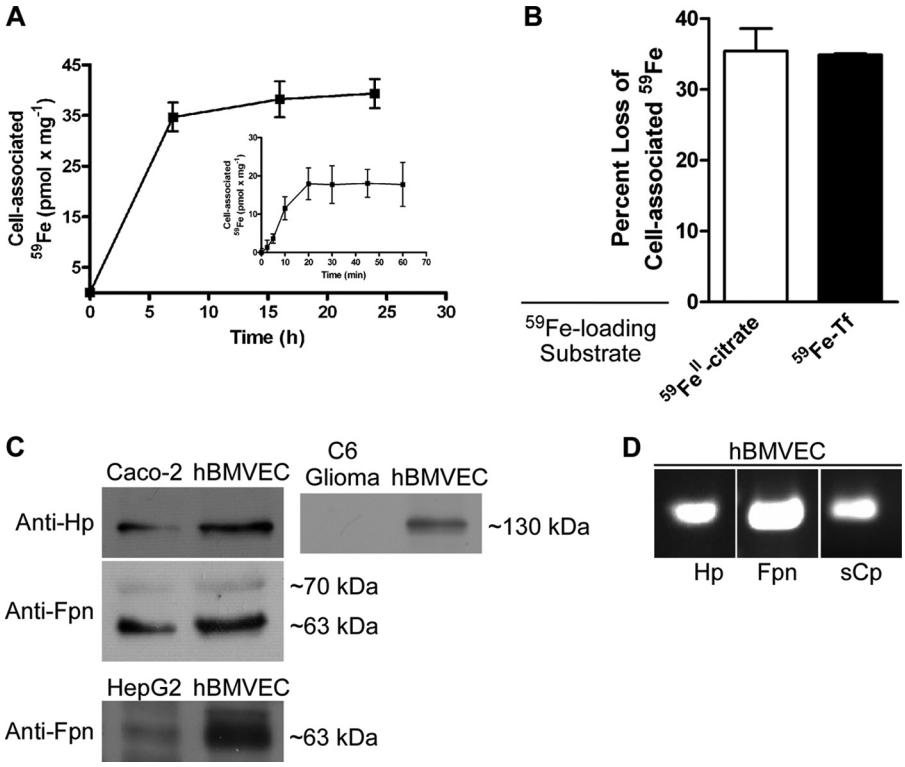

FIGURE 1. **hBMVEC, which express Hp, sCp, and Fpn, readily accumulate and efflux iron.** *A*, hBMVEC accumulation of 0.5 μM ^{59}Fe^{II} citrate plus ascorbate over a 24-h period. *Inset* illustrates the first 1 h of accumulation. Time 0 h is subtracted from all data points ($n = 6$, experimental replicates). *B*, ^{59}Fe efflux assays were performed using hBMVEC cell pellets loaded for 24 h with ^{59}Fe^{II} citrate plus ascorbate (*open*) or ^{59}Fe-Tf (*filled*). hBMVEC pellets were harvested after allowing 24 h for ^{59}Fe efflux. Data are represented as the percent loss of cell-associated ^{59}Fe with respect to time 0 h. Data are represented as means ± S.D. ($n = 4–8$, experimental replicates). *C*, immunoblots from whole cell lysates of C6 glioma, HepG2, Caco-2 cells, and hBMVEC were probed for either Hp or Fpn. Respective molecular weights are indicated to the right of the blots. Each lane was loaded with 20 μg of total protein. *D*, total RNA was collected from hBMVEC cells, and RT-PCR was performed to amplify Hp, Fpn, and Cp transcripts. Isoform-specific primers were used to amplify human soluble Cp from hBMVEC total RNA.

TABLE 1
Primer list used for RT-PCR

Transcript	Forward primer	Reverse primer
Hephaestin	GGATGCATGCAATCAATGG	CATCTTGAAAGGCTTCATATCG
Ferroportin	CAGGGACTGAGTGGTTCCAT	GGAGATTATGGGGACGGATT
Secreted (soluble) ceruloplasmin	TCCCTGGAACATACCAAACC	CCAATTTATTTCATTCAGCCGA

Hp, Fpn, and sCp Are Expressed by hBMVEC—The mechanism of cellular iron efflux from intestinal (21) and lens epithelial cells (22), macrophages (23), and oligodendrocytes (13) involves the functional cooperation of Fpn and an exocytoplasmic ferroxidase, either Hp or Cp. We propose that the same mechanism of iron efflux is true for hBMVEC. To test this, we first used Western blot to demonstrate expression of both Hp and Fpn as well as to establish the specificity of the antibodies, which we used throughout. The Caco-2 intestinal epithelial cell line was used as a positive control in our immunoblots. Caco-2 cells express both Hp and Fpn and have been established as a model for iron transport across the intestinal barrier (21, 24, 25). A distinct band at ~130 kDa is observed on immunoblots of Caco-2 and hBMVEC extracts probed for Hp; two distinct bands are observed at ~63 and 70 kDa when probed for Fpn (Fig. 1*C*). HepG2 cells were used as a negative control for Fpn antibody specificity in our immunoblots. HepG2 cells express minimal Fpn (26). As a negative control for Hp antibody, C6 glioma cells were used (Fig. 1*C*). Transcripts for both Hp and Fpn were also identified in hBMVEC via RT-PCR (Fig. 1*D*). Two isoforms of Cp have been identified in mammals, glycophosphatidylinositol-anchored Cp (GPI-Cp) and sCp. Further examination of the hBMVEC Cp message revealed that the transcript encoding sCp is expressed in this cell type (Fig. 1*D*). Primers used for RT-PCR are given in Table 1.

Hp and Fpn Are Co-localized to the Plasma Membrane of hBMVEC—We utilized indirect immunofluorescence with confocal microscopy to demonstrate subcellular localization of Hp and Fpn in hBMVEC monolayers. Both Fpn and Hp appear to be localized to the plasma membrane of hBMVEC; however, significant cytosolic staining of Fpn was observed in these cells as well (Fig. 2*A*). Merged images of Hp and Fpn demonstrated detectable co-localization of the two antigens in hBMVEC with this co-localization principally confined to the plasma membrane (Fig. 2*A*). High resolution images demonstrated that Hp presented with strict basolateral localization in the hBMVEC monolayers; in contrast, Fpn was visualized on both the cell surface and in the cytosol (Fig. 2*B*). Given the apparent diffuse Fpn localization in hBMVEC (Fig. 2*B*), we utilized HepG2 cells as a negative control for these indirect immunofluorescence

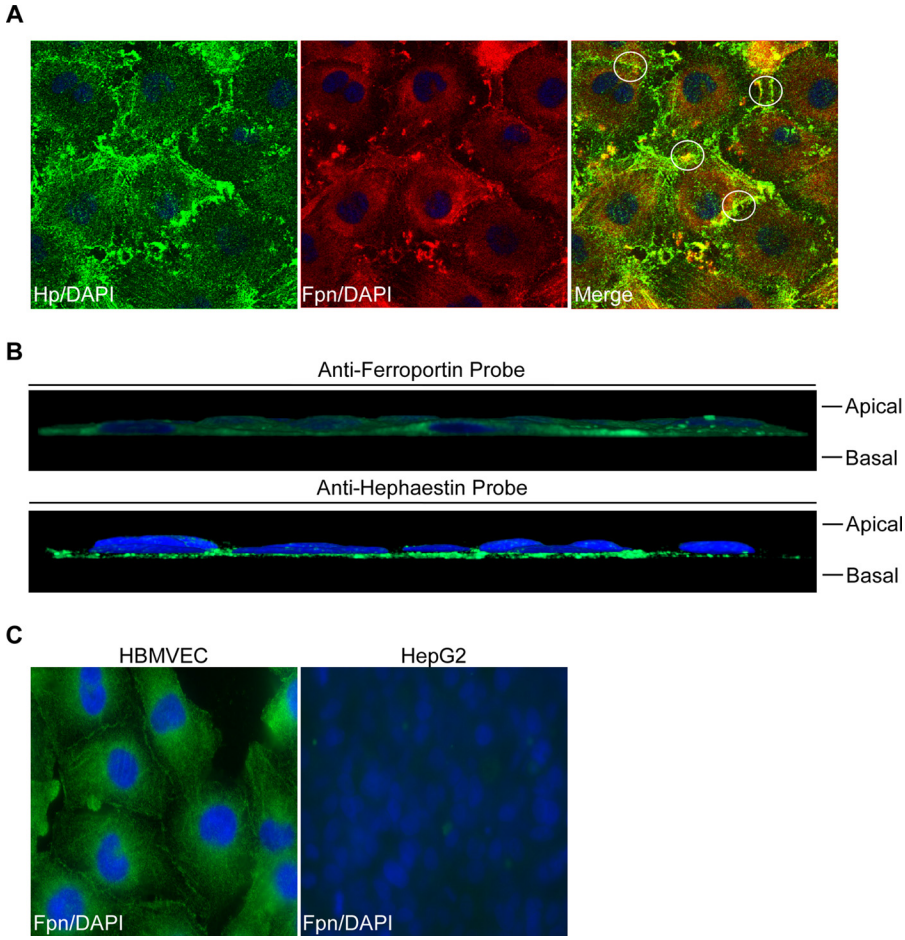

FIGURE 2. **Hp and Fpn are co-localized to the cell surface of hBMVEC.** *A*, hBMVEC monolayers were grown on glass coverslips and were processed for indirect immunofluorescence by confocal microscopy probing for Hp and Fpn. DAPI (*blue*) stains the nucleus. *Circles* highlight areas of Hp and Fpn co-localization in the merged image of hBMVEC. *B*, confocal microscopy performed on hBMVEC probed for Hp or Fpn was used to delineate polarized localization of these proteins. Side views demonstrate polarity in the case of Hp but not Fpn. Apical and basal surfaces are indicated to the *right* of the images. DAPI (*blue*) stains the nucleus. *C*, hBMVEC and HepG2 (negative control) monolayers were processed for indirect immunofluorescence probing for Fpn. DAPI (*blue*) stains the nucleus.

studies. Indeed, compared with the HepG2 control, the Fpn antibody specifically binds antigen on the hBMVEC plasma membrane (Fig. 2*C*).

Copper Chelation Depletes hBMVEC Hp Protein Abundance—To assess the contribution of Hp and/or sCp to hBMVEC iron efflux, we first stimulated the loss of ferroxidase *in vitro* by incubating hBMVEC with the copper chelating agent BCS (500 μM). Cellular copper depletion causes the loss of endogenous multicopper oxidase activity (8, 27). Comparison of indirect immunofluorescence images of BCS-treated to those of control cells indicated that the overall abundance of Hp in BCS-treated hBMVEC was decreased (Fig. 3*A*). To quantify the effect of BCS treatment on hBMVEC Hp expression, indirect immunofluorescence images taken from five separate fields of view were analyzed for their average fluorescent intensity. This analysis demonstrated that BCS-treated hBMVEC displayed decreased average fluorescence intensity when probed for Hp (Fig. 3*B*). As shown, there was a partial recovery of Hp after 48 h of BCS treatment. This pattern is addressed under the "Discussion."

hBMVEC Fpn Expression Is Decreased upon Loss of Endogenous Ferroxidase via BCS Treatment—In the absence of ferroxidase activity, *e.g.* with BCS treatment, Fpn is lost from the plasma membrane of cells (8, 27). Thus, we hypothesized that Fpn expression also would be diminished upon BCS treatment. BCS-treated and -untreated hBMVEC were probed for Fpn and analyzed via indirect immunofluorescence. Qualitative assessment of the images as above revealed a decrease in overall Fpn abundance in BCS-treated hBMVEC (Fig. 4*A*); quantitatively, the average fluorescent intensity of hBMVEC Fpn was significantly diminished as well (Fig. 4*D*). As observed for Hp, Fpn partially recovered 48h after treatment (Fig. 4*D*). The decrease in hBMVEC Fpn abundance upon treatment with BCS was confirmed by Western blot (Fig. 4*B*). In using BCS, of course, we cannot exclude the possibility that the effects on Fpn abundance are, to some extent, unrelated to the loss of cell Cp and Hp.

Addition of 6.6 nM soluble human plasma Cp (sCp) in the presence of BCS stabilized Fpn protein abundance in hBMVEC (Figs. 4*A* and 4*E*); this positive effect on Fpn due to added sCp was confirmed by Western blot (Fig. 4*B*). This concentration of sCp has been used previously to effectively stimulate iron efflux from cells depleted of their endogenous ferroxidase activity (7). In these experiments, sCp was added 24 h after BCS treatment was initiated to limit a possible thermal loss of sCp activity due to an extended incubation at 37 °C (28). The endogenous ferroxidase activity that was present in hBMVEC lysates was lost

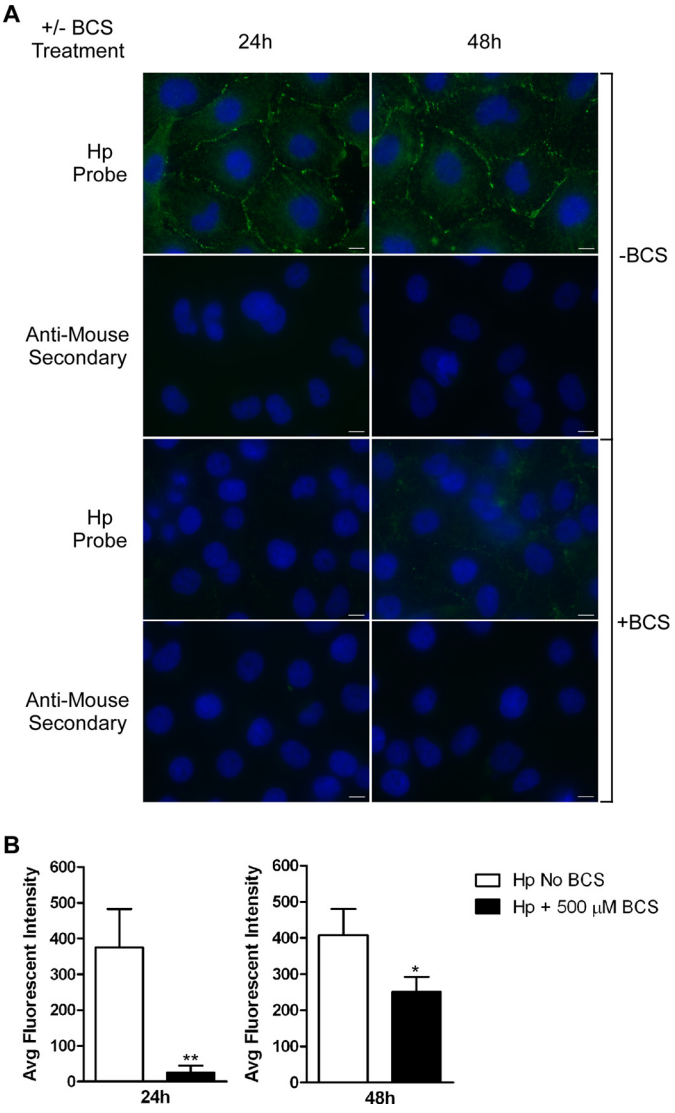

FIGURE 3. **Copper chelation depletes hBMVEC of endogenous Hp.** *A*, indirect immunofluorescence was used to investigate the abundance of Hp protein in BCS-treated and untreated hBMVEC. hBMVEC were treated with 500 μM BCS for 24–48 h. Secondary antibody only controls are shown. DAPI (*blue*) stains the nucleus. *Scale bar* represents 10 μm. *B*, average (*Avg*) fluorescent intensity from at least five separate fields of view were taken from each condition at each time point and were normalized for their respective secondary only control average fluorescent intensities. A series of paired *t* tests were used to analyze the data from each time point. *, $p < 0.05$ and **, $p < 0.005$. Data are represented as means ± S.D. ($n = 5$, technical replicates).

when hBMVEC were treated with BCS or BCS plus sCp for 24 h (Fig. 4*C*). These data suggest that the positive effect on Fpn due to sCp addition was correlated with the added sCp and not to a sCp-induced recovery of hBMVEC Hp.

Iron Efflux from hBMVEC Fpn Requires the Action of an Exocytoplasmic Ferroxidase—We hypothesized that depletion of Hp and sCp from hBMVEC due to BCS treatment would result in a reduced capacity for iron efflux. BCS has been used previously to knock down ferroxidase-catalyzed cellular iron mobilization (8). hBMVEC treated with 500 μM BCS and 0.5 μM $^{59}Fe^{II}$ citrate plus ascorbate retained more ^{59}Fe over 24 h than did BCS-untreated hBMVEC (Fig. 5*A*). Increased retention of ^{59}Fe in BCS-treated hBMVEC as compared with untreated hBMVEC was also observed when ^{59}Fe-Tf was used as substrate for loading (Fig. 5*B*). The increased cellular retention of ^{59}Fe in the presence of BCS could be due to either increased ^{59}Fe uptake or decreased ^{59}Fe efflux.

To delineate between these two potential mechanisms of hBMVEC ^{59}Fe retention, we utilized ^{59}Fe efflux assays along with BCS treatment. Treatment of hBMVEC with BCS resulted in the complete inhibition of ^{59}Fe efflux (Fig. 6*A*). Soluble Cp partially restored ^{59}Fe efflux from BCS-treated hBMVEC (Fig. 6*A*). BCS-treated hBMVEC loaded with ^{59}Fe-Tf exhibited a similar pattern of ^{59}Fe efflux; efflux was knocked down by BCS treatment with sCp supporting a 78% recovery (Fig. 6*B*). We infer from these data that BCS reduced the rate of ^{59}Fe efflux from hBMVEC rather than inhibiting iron uptake. Taken together, these data suggest that ^{59}Fe efflux from hBMVEC Fpn is potentiated by an exocytoplasmic ferroxidase regardless of its association with the plasma membrane, an effect likely associated with the restoration/stabilization of Fpn in the membrane. This pattern was the same whether TBI or NTBI was the ^{59}Fe source used to load the cells.

We next assessed the possible contribution of sCp secreted by hBMVEC to the stimulation of Fpn-dependent ^{59}Fe efflux. To do this, we applied fresh medium to a hBMVEC monolayer and incubated for 24 h to condition the media with the components of the hBMVEC secretome, including sCp. We collected the hBMVEC-conditioned media and applied it to BCS-treated hBMVEC, which had been loaded with $^{59}Fe^{II}$ citrate for 24 h. Efflux was monitored over 24 h in the continued presence of BCS. Indeed, although sCp restored efflux by 24% (Fig. 6*A*) hBMVEC-conditioned media also had a positive effect on iron efflux (13% recovery, Fig. 6*C*). These results suggest the likelihood that hBMVEC sCp does contribute to overall Fpn-dependent iron efflux from these cells.

DISCUSSION

In this work, we focused on the roles of Fpn and Hp in iron efflux from hBMVEC. Our first finding was that quantitatively, efflux and its dependence on a ferroxidase and Fpn are independent of the iron substrate (^{59}Fe-citrate or ^{59}Fe-Tf) used for hBMVEC ^{59}Fe loading. The data indicate that the ^{59}Fe obtained from these two substrates appears to follow the same efflux pathway in this model system. The most significant result shown is that efflux from BCS-treated cells loaded with ^{59}Fe-Tf exhibit no iron efflux. Thus, at least in the experimental paradigm described here, we found no evidence for detectable ^{59}Fe-Tf recycling.

Iron efflux in mammals generally occurs via the cooperation of Fpn and a multicopper oxidase. Both Fpn and the ferroxidase Hp have been identified at the transcript and protein level in BMVEC (5, 6). We confirmed these observations in our hBMVEC model system (Figs. 1 and 2). Furthermore, we demonstrated that Hp and Fpn are colocalized to the plasma membrane of hBMVEC, an observation that correlates with the bulk of the literature regarding Hp and Fpn subcellular localization (11).

Cooperation of Fpn and Hp in supporting iron export from cells endogenous to the CNS has been demonstrated previously (13, 29). Here, we have presented evidence that Fpn and Hp cooperate in the process by which iron is released from the

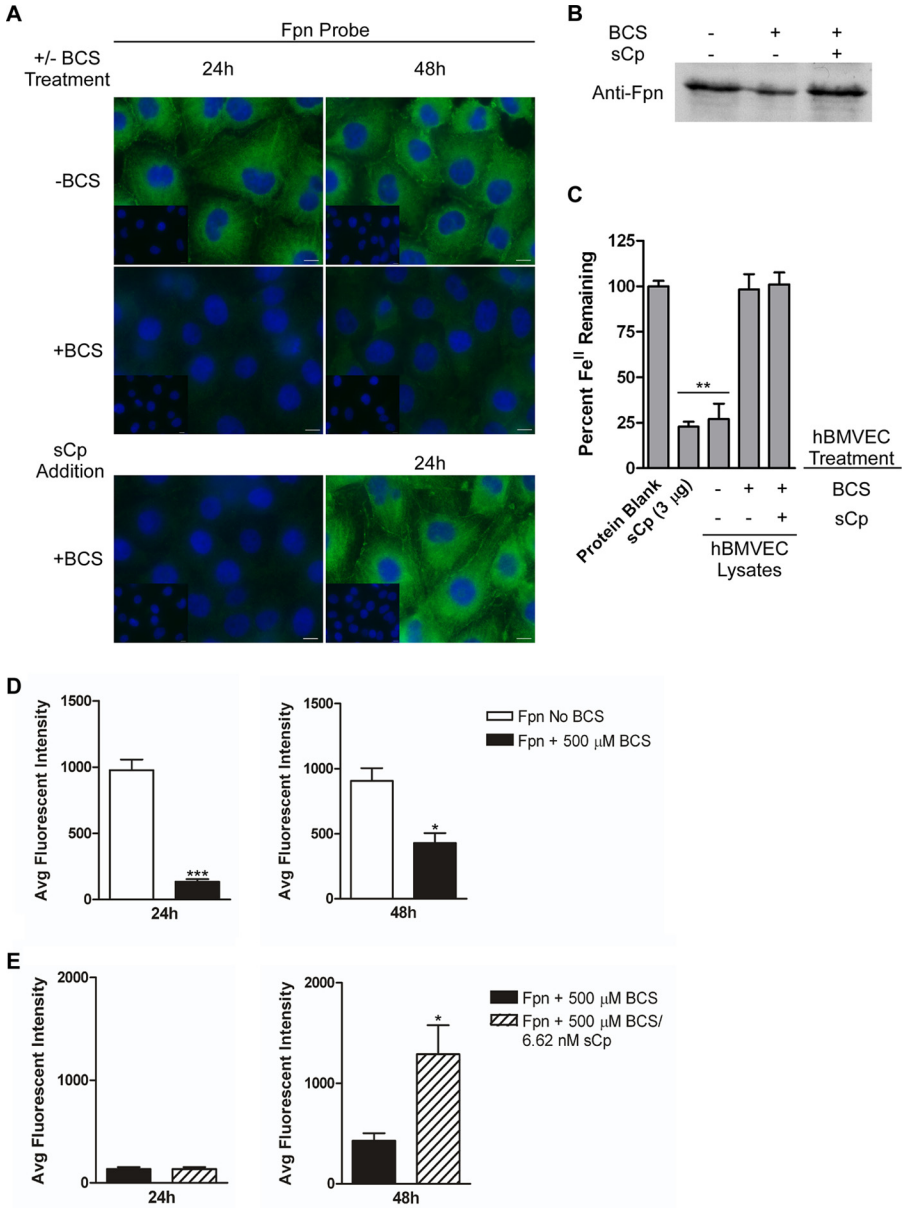

FIGURE 4. **Exocytoplasmic ferroxidase activity stabilizes hBMVEC Fpn but not Hp abundance in the presence of BCS.** *A*, indirect immunofluorescence was used to investigate the abundance of Fpn protein in BCS-treated and untreated hBMVEC. hBMVEC were treated with 500 μM BCS for 24–48 h. Additionally, recovery of Fpn protein abundance in BCS-treated hBMVEC by ferroxidase-active sCp (6.6 nM) was investigated. Fresh sCp was added to media during the final 24 h of BCS treatment. *Insets* depict secondary antibody only controls. DAPI (*blue*) stains the nucleus. *Scale bar* represents 10 μm. *B*, immunoblot depicting Fpn abundance in hBMVEC lysates (20 μg of protein per lane). hBMVEC were incubated for 24 h without BCS, with BCS, or with BCS plus sCp (6.6 nM) for an additional 24 h before lysis. *C*, ferroxidase assays were used to investigate the abundance of endogenous ferroxidase activity in hBMVEC lysates. hBMVEC were treated for 24 h without BCS, with BCS, or with BCS plus sCp (6.6 nM) for an additional 24 h. Ferroxidase activity is indicated by the fraction of Fe^{II} remaining as detected by formation of the Fe(II)-ferrozine complex ($n = 3$, experimental replicates). *D* and *E*, samples from *A* were used to quantify average fluorescent intensities from at least five separate fields of view from each condition at each time point and were normalized for their respective secondary only control average fluorescent intensities. Significance of the data (*C*) was assessed using one-way analysis of variance parameters. A series of paired *t* tests were used to analyze the data from each time point in *D* and *E*. *, $p < 0.005$; **, $p < 0.001$; ***, $p < 0.0001$. Data are represented as means ± S.D. (*A*, *D*, and *E*, $n = 5$, technical replicates).

barrier cells of the brain, the BMVEC; note that the polarity of this efflux could not be determined in our monolayer system. We have investigated the roles of Hp, sCp, and Fpn in hBMVEC iron efflux using the copper-chelating agent BCS. Decreased intracellular copper levels results in an increase in the turnover of mature endogenous Hp due to an abrogation of copper incorporation into the newly synthesized protein (30). Examination of rats with perinatal copper deficiency revealed decreased plasma and brain iron concentrations as compared with copper sufficient controls, indicating a role for multicopper oxidases in systemic iron trafficking (31).

In the absence of a ferroxidase (via BCS treatment), there is a reported hepcidin-independent internalization of Fpn from the cell surface of both HeLa and C6 glioma cells (8, 27). In glioma cells, the ferroxidase lost is GPI-linked Cp. This effect has been paired with a loss in iron efflux from these cells (8). Here, we have shown Hp and Fpn depletion from BCS-treated hBMVEC via quantification of the relative

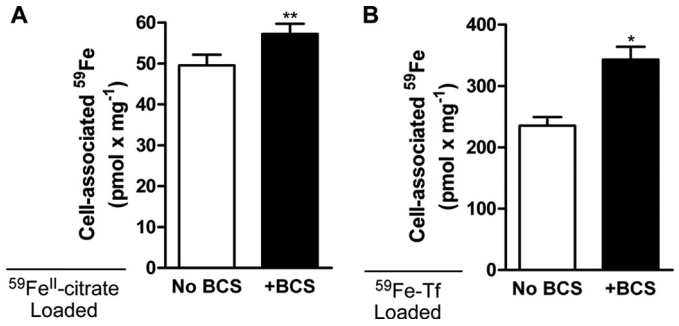

FIGURE 5. **Copper chelation increases hBMVEC iron retention.** *A*, hBMVEC-associated ^{59}Fe after loading for 24 h with 0.5 μM ^{59}Fe^{II} citrate plus ascorbate in the presence or absence of 500 μM BCS. *B*, hBMVEC-associated ^{59}Fe after loading for 24 h with ^{59}Fe-Tf plus citrate in the presence or absence of 500 μM BCS. A series of paired *t* tests were used to analyze the data. *, $p < 0.05$ and **, $p < 0.005$. Data are represented as means ± S.D. ($n = 4–8$, experimental replicates).

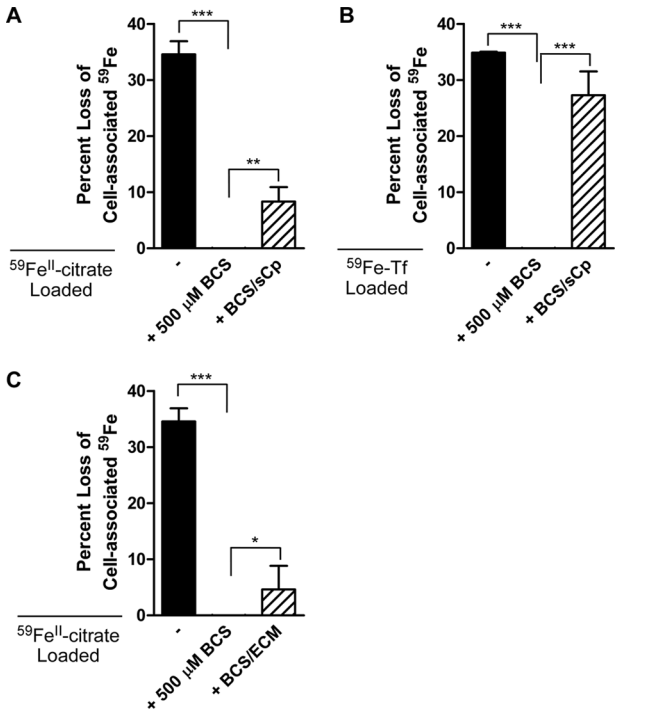

FIGURE 6. **hBMVEC iron efflux inhibited by BCS treatment can be restored via the addition of exogenous sCp or hBMVEC-conditioned media.** *A*, ^{59}Fe efflux assays were performed on hBMVEC loaded with ^{59}Fe^{II} citrate plus ascorbate. ^{59}Fe efflux assays were also performed using BCS-treated hBMVEC in the presence or absence of ferroxidase active sCp (6.6 nM) added at the beginning of the 24 h efflux assay. *B*, ^{59}Fe efflux assays were performed on hBMVEC loaded with ^{59}Fe-Tf plus citrate. ^{59}Fe efflux assays were also performed using BCS-treated hBMVEC in the presence or absence of ferroxidase active sCp (6.6 nM) added at the beginning of the 24 h efflux assay. *C*, ^{59}Fe efflux assays were performed on hBMVEC loaded with ^{59}Fe^{II} citrate plus ascorbate. Efflux activity was partially recovered via the addition of hBMVEC-conditioned media (*ECM*) to BCS-treated hBMVEC. All BCS values were not statistically different than zero. Significance was determined for each set of data using one-way analysis of variance analysis. *, $p < 0.05$; **, $p < 0.01$; and **, $p < 0.001$. Data are represented as means ± S.D. ($n = 4–8$, experimental replicates).

fluorescent intensity of indirect immunofluorescent images (Figs. 3 and 4); a loss in BCS-treated hBMVEC ^{59}Fe-efflux was also observed (Fig. 6).

Ferroportin mRNA contains a 5′-UTR iron-responsive element (32). Binding of the iron regulatory protein 1 to the iron-responsive element under low cytosolic iron conditions post-transcriptionally regulates the expression of Fpn by repressing the translation initiation of the transcript (33). Under conditions of high intracellular iron, as created by the inhibition of iron efflux activity via BCS treatment, the iron regulatory protein no longer associates with the Fpn iron-responsive element, allowing for translation initiation of the transcript. Although Fpn protein is turned over in the absence of a ferroxidase (8, 27), the increased translation initiation of the transcript may account for the subtle recovery of hBMVEC Fpn seen after 48 h of BCS treatment (Fig. 4). Increased turnover of Fpn in the absence of a ferroxidase does not mean that newly synthesized protein is not trafficked to the membrane; the increased turnover results from internalization due to increased ubiquitination (34).

The loss of Fpn protein in C6 glioma cells depleted of ferroxidase activity (GPI-Cp) can be reversed via the addition of exogenous ferroxidase activity (8). The most likely candidate ferroxidase in the blood and interstitial spaces of the brain is sCp. Soluble Cp in the blood is secreted primarily by hepatocytes (35). We have demonstrated that sCp transcript is present in hBMVEC (Fig. 1*D*). This is the first example of Cp message in the endothelial cells of the BBB; this result suggests that BMVEC may be a source of brain sCp.

Soluble Cp exists in concentrations ranging from 1.6–3.4 μM in the blood and 5.8–6.8 nM in the cerebrospinal fluid (12). A concentration of 6.6 nM sCp, the concentration we have used here, effectively stimulates iron efflux from cells depleted of their endogenous ferroxidase activity (7). At this concentration, sCp significantly increased the abundance of Fpn protein in BCS-treated hBMVEC (Fig. 4). The restoration of hBMVEC Fpn protein abundance in conjunction with the ferroxidase activity provided by sCp significantly increased the ability of BCS-treated hBMVEC to efflux ^{59}Fe (Fig. 6); such activity was also provided by hBMVEC-secreted sCp (Fig. 6*C*). Our data suggest that Fpn and exocytoplasmic ferroxidase activity are required for ^{59}Fe efflux from hBMVEC. This ferroxidase activity can be provided by either a cell endogenous (Hp) or exogenous (sCp) ferroxidase protein.

Soluble Cp more effectively stimulated iron efflux from hBMVEC loaded with iron-Tf than with iron citrate (Fig. 6). This difference may be due to the fact that more iron is accumulated and retained in hBMVEC when loaded with Tf-iron than iron citrate, thus creating an iron gradient within the cells (Fig. 5). This gradient provides a stronger driving force for efflux initiated upon the recovery of Fpn due to the addition of exogenous sCp.

Functionally, Cp protein in the CNS and in the peripheral circulation is similar; however, in the brain and a few other tissues, a post-translational modification yields a GPI anchor that attaches the protein to the extracellular surface of the cell in which it is expressed (36–38). In the CNS, GPI-Cp is highly concentrated to astrocytes (15, 36, 39) where an interaction with Fpn has been observed (7); the majority of these astrocytes neighbor BMVEC (39, 40). We demonstrated that sCp can stimulate hBMVEC ^{59}Fe efflux (Fig. 6). Our data suggest the possibility that in the intact brain, astrocyte GPI-Cp or BMVEC sCp could support iron efflux through Fpn even in the absence of BMVEC Hp as seen in the *sla*$^{-/-}$ mouse in which iron accu-

mulation is observed in oligodendrocytes (9, 13). This hypothesis is the subject of ongoing research.

In addition to suggesting a mechanism for iron efflux from hBMVEC, we have presented several interesting observations that contribute broadly to the field of brain iron accumulation. First, we have presented data that suggest the main iron substrate for hBMVEC is Tf-iron, which is retained by hBMVEC in nearly a 5-fold excess to non-Tf bound iron (Fig. 5). Second, our data strongly suggest that iron is released from Tf-iron, likely via the canonical transferrin receptor cycling pathway, before exiting the cell as "free" iron. Thus, our results are not easily reconciled with the proposition that a major fraction of brain iron uptake is supported by a holo-Tf transcytosis pathway through these endothelial cells (18, 19). Experiments in a Transwell model of the BBB will be required to specifically examine this transcytosis mechanism.

Acknowledgments—We thank Dr. Supriya Mahajan for generous donation of hBMVEC. We acknowledge the assistance of Dr. Wade Sigurdson at the Confocal Microscope and Flow Cytometry Facility in the School of Medicine and Biomedical Sciences (University at Buffalo).

REFERENCES

1. Salvador, G. A. (2010) Iron in neuronal function and dysfunction. *BioFactors* **36,** 103–110
2. Todorich, B., Pasquini, J. M., Garcia, C. I., Paez, P. M., and Connor, J. R. (2009) Oligodendrocytes and myelination: The role of iron. *Glia* **57,** 467–478
3. Ganz, T. (2005) Cellular iron: ferroportin is the only way out. *Cell Metab.* **1,** 155–157
4. Donovan, A., Brownlie, A., Zhou, Y., Shepard, J., Pratt, S. J., Moynihan, J., Paw, B. H., Drejer, A., Barut, B., Zapata, A., Law, T. C., Brugnara, C., Lux, S. E., Pinkus, G. S., Pinkus, J. L., Kingsley, P. D., Palis, J., Fleming, M. D., Andrews, N. C., and Zon, L. I. (2000) Positional cloning of zebrafish ferroportin1 identifies a conserved vertebrate iron exporter. *Nature* **403,** 776–781
5. Wu, L. J., Leenders, A. G., Cooperman, S., Meyron-Holtz, E., Smith, S., Land, W., Tsai, R. Y., Berger, U. V., Sheng, Z. H., and Rouault, T. A. (2004) Expression of the iron transporter ferroportin in synaptic vesicles and the blood-brain barrier. *Brain Res.* **1001,** 108–117
6. Yang, W., Jung, K., Lee, M., Lee, Y., Nakagawa, S., Niwa, M., Cho, S., and Kim, D. (2011) Transient expression of iron transport proteins in the capillary of the developing rat brain. *Cell Mol. Neurobiol.* **31,** 93–99
7. Jeong, S. Y., and David, S. (2003) Glycosylphosphatidylinositol-anchored ceruloplasmin is required for iron efflux from cells in the central nervous system. *J. Biol. Chem.* **278,** 27144–27148
8. De Domenico, I., Ward, D. M., di Patti, M. C., Jeong, S. Y., David, S., Musci, G., and Kaplan, J. (2007) Ferroxidase activity is required for the stability of cell surface ferroportin in cells expressing GPI-ceruloplasmin. *EMBO J.* **26,** 2823–2831
9. Vulpe, C. D., Kuo, Y. M., Murphy, T. L., Cowley, L., Askwith, C., Libina, N., Gitschier, J., and Anderson, G. J. (1999) Hephaestin, a ceruloplasmin homologue implicated in intestinal iron transport, is defective in the sla mouse. *Nat. Genet.* **21,** 195–199
10. De Domenico, I., Ward, D. M., Langelier, C., Vaughn, M. B., Nemeth, E., Sundquist, W. I., Ganz, T., Musci, G., and Kaplan, J. (2007) The molecular mechanism of hepcidin-mediated ferroportin down-regulation. *Mol. Biol. Cell* **18,** 2569–2578
11. Han, O., and Kim, E. Y. (2007) Colocalization of ferroportin-1 with hephaestin on the basolateral membrane of human intestinal absorptive cells. *J. Cell Biochem.* **101,** 1000–1010
12. Gaasch, J. A., Lockman, P. R., Geldenhuys, W. J., Allen, D. D., and Van der Schyf, C. J. (2007) Brain iron toxicity: differential responses of astrocytes, neurons, and endothelial cells. *Neurochem. Res.* **32,** 1196–1208
13. Schulz, K., Vulpe, C. D., Harris, L. Z., and David, S. (2011) Iron efflux from oligodendrocytes is differentially regulated in gray and white matter. *J. Neurosci.* **31,** 13301–13311
14. Greco, T. M., Seeholzer, S. H., Mak, A., Spruce, L., and Ischiropoulos, H. (2010) Quantitative mass spectrometry-based proteomics reveals the dynamic range of primary mouse astrocyte protein secretion. *J. Proteome Res.* **9,** 2764–2774
15. Patel, B. N., and David, S. (1997) A novel glycosylphosphatidylinositol-anchored form of ceruloplasmin is expressed by mammalian astrocytes. *J. Biol. Chem.* **272,** 20185–20190
16. Qian, Z. M., Chang, Y. Z., Zhu, L., Yang, L., Du, J. R., Ho, K. P., Wang, Q., Li, L. Z., Wang, C. Y., Ge, X., Jing, N. L., Li, L., and Ke, Y. (2007) Development and iron-dependent expression of hephaestin in different brain regions of rats. *J. Cell Biochem.* **102,** 1225–1233
17. Greenough, M. A., Camakaris, J., and Bush, A. I. (2013) Metal dyshomeostasis and oxidative stress in Alzheimer's disease. *Neurochem. Int.* **62,** 540–555
18. Skjørringe, T., Møller, L. B., and Moos, T. (2012) Impairment of interrelated iron- and copper homeostatic mechanisms in brain contributes to the pathogenesis of neurodegenerative disorders. *Front. Pharmacol.* **3,** 169
19. Moos, T., Rosengren Nielsen, T., Skjørringe, T., and Morgan, E. H. (2007) Iron trafficking inside the brain. *J. Neurochem.* **103,** 1730–1740
20. McCarthy, R. C., and Kosman, D. J. (2012) Mechanistic analysis of iron accumulation by endothelial cells of the BBB. *Biometals* **25,** 665–675
21. Chen, H., Attieh, Z. K., Dang, T., Huang, G., van der Hee, R. M., and Vulpe, C. (2009) Decreased hephaestin expression and activity leads to decreased iron efflux from differentiated Caco2 cells. *J. Cell Biochem.* **107,** 803–808
22. Wolkow, N., Song, D., Song, Y., Chu, S., Hadziahmetovic, M., Lee, J. C., Iacovelli, J., Grieco, S., and Dunaief, J. L. (2012) Ferroxidase hephaestin's cell-autonomous role in the retinal pigment epithelium. *Am. J. Pathol.* **180,** 1614–1624
23. Anderson, G. J., and Vulpe, C. D. (2009) Mammalian iron transport. *Cell Mol. Life Sci.* **66,** 3241–3261
24. Thomas, C., and Oates, P. S. (2004) Ferroportin/IREG-1/MTP-1/SLC40A1 modulates the uptake of iron at the apical membrane of enterocytes. *Gut.* **53,** 44–49
25. Chung, B., Chaston, T., Marks, J., Srai, S. K., and Sharp, P. A. (2009) Hepcidin decreases iron transporter expression *in vivo* in mouse duodenum and spleen and *in vitro* in THP-1 macrophages and intestinal Caco-2 cells. *J. Nutr.* **139,** 1457–1462
26. Marques, L., Auriac, A., Willemetz, A., Banha, J., Silva, B., Canonne-Hergaux, F., and Costa, L. (2012) Immune cells and hepatocytes express glycosylphosphatidylinositol-anchored ceruloplasmin at their cell surface. *Blood Cells Mol. Dis.* **48,** 110–120
27. Kono, S., Yoshida, K., Tomosugi, N., Terada, T., Hamaya, Y., Kanaoka, S., and Miyajima, H. (2010) Biological effects of mutant ceruloplasmin on hepcidin-mediated internalization of ferroportin. *Biochim. Biophys. Acta* **1802,** 968–975
28. Sedlák, E., Žoldák, G., and Wittung-Stafshede, P. (2008) Role of copper in thermal stability of human ceruloplasmin. *Biophys. J.* **94,** 1384–1391
29. Wang, J., Jiang, H., and Xie, J. X. (2007) Ferroportin1 and hephaestin are involved in the nigral iron accumulation of 6-OHDA-lesioned rats. *Eur. J. Neurosci.* **25,** 2766–2772
30. Nittis, T., and Gitlin, J. D. (2004) Role of copper in the proteosome-mediated degradation of the multicopper oxidase hephaestin. *J. Biol. Chem.* **279,** 25696–25702
31. Prohaska, J. R., and Gybina, A. A. (2005) Rat brain iron concentration is lower following perinatal copper deficiency. *J. Neurochem.* **93,** 698–705
32. Abboud, S., and Haile, D. J. (2000) A novel mammalian iron-regulated protein involved in intracellular iron metabolism. *J. Biol. Chem.* **275,** 19906–19912
33. Leipuviene, R., and Theil, E. (2007) The family of iron responsive RNA structures regulated by changes in cellular iron and oxygen. *Cell Mol. Life Sci.* **64,** 2945–2955
34. Qiao, B., Sugianto, P., Fung, E., Del-Castillo-Rueda, A., Moran-Jimenez,

M. J., Ganz, T., and Nemeth, E. (2012) Hepcidin-induced endocytosis of ferroportin is dependent on ferroportin ubiquitination. *Cell Metab.* **15,** 918–924
35. Slany, A., Haudek, V. J., Zwickl, H., Gundacker, N. C., Grusch, M., Weiss, T. S., Seir, K., Rodgarkia-Dara, C., Hellerbrand, C., and Gerner, C. (2010) Cell characterization by proteome profiling applied to primary hepatocytes and hepatocyte cell lines Hep-G2 and Hep-3B. *J. Proteome Res.* **9,** 6–21
36. Patel, B. N., Dunn, R. J., and David, S. (2000) Alternative RNA splicing generates a glycosylphosphatidylinositol-anchored form of ceruloplasmin in mammalian brain. *J. Biol. Chem.* **275,** 4305–4310
37. Rouault, T. A., and Cooperman, S. (2006) Brain iron metabolism. *Semin. Pediatr. Neurol.* **13,** 142–148
38. Dringen, R., Bishop, G. M., Koeppe, M., Dang, T. N., and Robinson, S. R. (2007) The pivotal role of astrocytes in the metabolism of iron in the brain. *Neurochem. Res.* **32,** 1884–1890
39. Klomp, L. W., Farhangrazi, Z. S., Dugan, L. L., and Gitlin, J. D. (1996) Ceruloplasmin gene expression in the murine central nervous system. *J. Clin. Invest.* **98,** 207–215
40. Klomp, L. W., and Gitlin, J. D. (1996) Expression of the ceruloplasmin gene in the human retina and brain: Implications for a pathogenic model in Aceruloplasminemia. *Hum. Mol. Genet.* **5,** 1989–1996